doi:10.1017/S1431927622004743
Microsc. Microanal. 28 (Suppl 1), 2022

Visualizing the Macro- and Micronutrient Distribution of Toxic Cyanobacteria in Two and Three Dimensions

Bobby G. Duersch[1], Yanqi Luo[2], Si Chen[2], Steven A. Soini[1], Dawn M. Raja Somu[1] and Vivian M. Merk[1*]

[1.] Department of Chemistry and Biochemistry, Florida Atlantic University, Boca Raton, FL, USA.
[2.] Advanced Photon Source, Argonne National Laboratory, Argonne, IL, USA.
* Corresponding author: vmerk@fau.edu

Cyanobacteria, also called blue-green algae, are an ancient group of prokaryotic microbes. In abundance, these aquatic microorganisms can produce Harmful Algal Blooms (HAB) that impair human health and aquatic ecosystems around the world. Eutrophication, the excessive supply of macronutrients, such as nitrates or phosphates, promotes the occurrence of HAB, which release hazardous cyanotoxins into affected waterbodies. Recent studies have shown that the production of microcystin toxins is triggered by iron depletion, but little is known about the effect of other trace elements. This study quantified the effect of micronutrients on the growth of the freshwater cyanobacteria *Microcystis aeruginosa* (*M. aeruginosa*), their photosynthetic activity and cyanotoxin production at the cellular and organelle level. Towards this goal, we quantitatively mapped the spatial and cellular content of various metals (Zn, Cu, Fe, and Mn) and macronutrients (K, Ca, and P) across the ultrastructure of frozen-hydrated single cells using state-of-the-art synchrotron X-ray nanofluorescent (SR-XRF) imaging at the Advanced Photon Source (APS) at Argonne National Laboratory. The cryogenic capabilities at beamline 9-ID-B are ideal for visualizing the ultrastructure of aquatic microorganisms in their near-native state, thereby avoiding the invasive process of embedding. High-speed freezing is the method of choice to preserve the cellular integrity by avoiding ice crystal formation.

Mapping the spatial distribution and quantification of trace elements within *M. aeruginosa* cells provided valuable insights in addition to global elemental information from microwave plasma optical emission spectrometry (MP-OES). A unique advantage of elemental imaging with the Bionanoprobe at beamline 9-ID-B is the sub-100nm spatial resolution and high chemical sensitivity towards multiple trace elements [2]. This experimental technique has rarely been used for imaging planktonic organisms [4]. The use of the SR-XRF bears remarkable scientific potential due to the non-destructive nature, nanometer spatial resolution and high penetrating capabilities of X-rays [10].

Cyanobacteria were collected in Lake Okeechobee, Florida, and maintained in BG-11 culture medium, allowing us to study the influence of micronutrients on cyanobacterial population dynamics in subtropical climates. 2% dimethyl sulfoxide (DMSO) was added to the samples as cryoprotectant. Due to their small cell diameter of 3-4µm, *M. aeruginosa* cells were vitrified by plunge freezing. Live cells were drop-cast onto low stress SiN_x windows. Excess water was blotted off prior to plunge freezing in liquid nitrogen. The SiN_x windows were kept in customized holders at -196°C and shipped to the beamline.

Scanning X-ray fluorescence data were collected in combination with differential phase-contrast images at the 9-ID-B,C end station (Xradia Bionanoprobe) [2] with an incident photon energy of 10.0 keV. Entire X-ray fluorescence spectra were acquired for each pixel using a collimated four-element Si-drift

detector. Detected elements include Z = 13 (Al) – Z = 30 (Zn), specifically P, S, K, Ca, Cr, Mn, Fe, Co, Ni, Cu, and Zn. Target cells were located using a Nikon light microscope installed at the beamline. Radiometric scans were collected with a step size down to 65nm. The background was approximated using a peak stripping algorithm. Spectral peaks were fit to an exponentially modified Gaussian curve to determine the peak areas in accordance with fixed ratios of the K_α and K_β peak areas. Elemental mappings and three-color colocalization mappings were generated using the MAPS-software [11]. X-ray fluorescence counts were converted to area concentrations (g cm^{-2}) using peak area to concentration ratios determined from NIST thin-film standards and displayed with varying concentration scales. Cellular-level elemental concentrations (g μm^2) were determined by defining regions of interest (ROI) around the circumference of the cell using the MAPS software [7]. Elemental concentrations in specific areas were determined using the region of interest (ROIs) feature in the MAPS software [11]. A tomographic dataset was obtained from a total of 54 projections with 80 nm step size. The 3D tomographic reconstruction of four cells was done using a SIRT algorithm in the ASTRA toolbox [8]. The Tomviz software package was used for visualizing the 3D volumetric dataset [6].

Fig. 1 displays the spatial distribution for the elements P, S, K, Ca, Fe, Cu, and Zn in a representative group of four cells. The trace elements Fe, Zn and Cu are homogeneously distributed across the cyanobacterial cells. Elevated Ca concentrations are found along the nuclear fission line of two dividing cells. Strikingly, intracellular P and K are co-localized as discrete clusters. These P/K hotspots have a mean diameter of 0.45 ± 0.05 µm and a mean concentration of 3.0 ± 0.4 µg/cm^2 (P) and 2.0 ± 0.3 µg/cm^2 (K), respectively, over twice as much as compared to the average P and K content in the rest of the cell. Previous studies reported on P hotspots colocalized with Ca and Fe in eukaryotic *Chlorella* sp. and *Chlamydomonas* sp. algae [3].

While achieving high spatial resolution, 2D projected elemental mappings are not suitable for visualizing the three-dimensional (3D) arrangement of the elements, which is vital for identifying cellular organelles, such as thylakoids and gas vesicles [5]. Thus, we employed non-destructive X-ray fluorescence nanotomography to explore the 3D elemental distribution in the group of four individual cells (Fig. 2). The tomographic dataset illustrates elongated polyphosphate bodies surrounded by K envelopes.

In summary, X-ray fluorescence nanotomography is vital for understanding the role macro- and micronutrients play within a *M. aeruginosa* cell [1]. Studying the quantitative elemental distribution and colocalization in cyanobacteria is crucial to identify the mechanisms that macro- and micronutrients play in proliferation and toxin production. Thus, multimodal X-ray imaging provides us with a better understanding of intracellular biochemical processes of cyanobacteria, helping us monitor and combat an emerging environmental threat [12].

https://doi.org/10.1017/S1431927622004743 Published online by Cambridge University Press

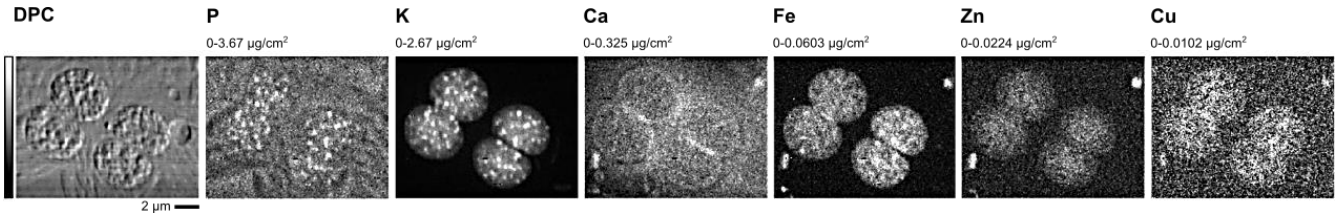

Figure 1. Synchrotron XRF micrograph of frozen-hydrated *Microcystis aeruginosa* cells obtained with Bionanoprobe (Advanced Photon Source). Elemental mapping shows homogeneous distribution of Fe, Zn, and Cu, and co-localization of P and K in hotspots. Differential phase contrast (DPC) imaging provides the cellular ultrastructure.

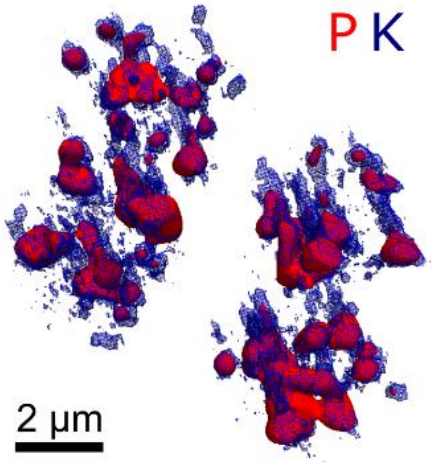

Figure 2. Cryo 3D X-ray fluorescence nanotomographic dataset from group of four *Microcystis aeruginosa* cells. Phosphorus (P) is red and potassium (K) is blue.

References:

[1] S Chen et al., SPIE Optical Engineering + Applications (2015), 95920I. doi:10.1117/12.2190672
[2] S Chen et al., J. Synchrotron Radiation. **21**(1) (2014), p. 66. doi:10.1107/S1600577513029676
[3] J Diaz et al., Limnol. Oceanogr. Methods **7**(1) (2009), p. 42. doi:10.4319/lom.2009.7.42
[4] MD De Jonge and S Vogt, Curr. Opin. Struct. Biol. **20**(5) (2010), p. 606. doi:10.1016/j.sbi.2010.09.002
[5] D Junjing et al., Sci. Adv. **4**(11) (2021), p. eaau4548. doi:10.1126/sciadv.aau4548
[6] B Levin et al., Micros. Today **26**(1) (2018), p. 12. doi:10.1017/S1551929517001213
[7] T Nietzold et al., J Vis Exp **132** (2018), p. 56042. doi:10.3791/56042
[8] WJ Palenstijn et al., Adv. Struct. Chem. Imaging **2**(1) (2016). doi:10.1186/s40679-016-0032-z
[9] MJ Rastoll et al., J. Appl. Phycol. **25**(5) (2013), p. 1483. doi:10.1007/s10811-013-0001-z
[10] BS Twining et al., Anal. Chem. **75**(15) (2003), p. 3806. doi:10.1021/ac034227z
[11] S Vogt et al., J. Phys. IV Fr. **104** (2003), p. 635. doi:10.1051/JP4:20030160
[12] The authors acknowledge funding from the Walter and Lalita Janke foundation Innovations in Sustainability Science Research Grant to Dr. Merk. This research used resources of the Advanced

Photon Source; a U.S. Department of Energy (DOE) Office of Science User Facility operated for the DOE Office of Science by Argonne National Laboratory under Contract No. DE-AC02-06CH11357.